

# Time-resolved x-ray diffraction and calorimetric studies at low scan rates

## II. On the fine structure of the phase transitions in hydrated dipalmitoylphosphatidylethanolamine

Haruhiko Yao, Ichiro Hatta, Rumiana Koynova,\* and Boris Tenchov\*

Department of Applied Physics, School of Engineering, Nagoya University, Chikusa-ku, Nagoya 464-01, Japan;  
and \*Central Laboratory of Biophysics, Bulgarian Academy of Sciences, 1113 Sofia, Bulgaria

**ABSTRACT** The phase transitions of dipalmitoylphosphatidylethanolamine (DPPE) in excess water have been examined by low-angle time-resolved x-ray diffraction and calorimetry at low scan rates. The lamellar subgel/lamellar liquid-crystalline ( $L_c \rightarrow L_\alpha$ ), lamellar gel/lamellar liquid-crystalline ( $L_\beta \rightarrow L_\alpha$ ), and lamellar liquid-crystalline/lamellar gel ( $L_\alpha \rightarrow L_\beta$ ) phase transitions proceed via coexistence of the initial and final phases with no detectable intermediates at scan rates 0.1 and 0.5°C/min. At constant temperature within the region of the  $L_\beta \rightarrow L_\alpha$  transition the ratio of the two coexisting phases was found to be stable for over 30 min. The state of stable phase coexistence was preceded by a 150-s relaxation taking place at constant temperature after termination of the heating scan in the transition region. While no intermediate structures were present in the coexistence region, a well reproducible multipeak pattern, with at least four prominent heat capacity peaks separated in temperature by 0.4–0.5°C, has been observed in the cooling transition ( $L_\alpha \rightarrow L_\beta$ ) by calorimetry. The multipeak pattern became distinct with an increase of incubation time in the liquid-crystalline phase. It was also clearly resolved in the x-ray diffraction intensity versus temperature plots recorded at slow cooling rates. These data suggest that the equilibrium state of the  $L_\alpha$  phase of hydrated DPPE is represented by a mixture of domains that differ in thermal behavior, but cannot be distinguished structurally by x-ray scattering.

## INTRODUCTION

Due to their frequent occurrence in biological membranes phosphatidylethanolamines (PEs) have received much attention in model studies. Similarly to other lipid-water systems, their dispersions in water display rich polymorphism at variations of water content, temperature, thermal prehistory, and concentration of other solutes. Saturated PEs can form several different phases in excess water: lamellar subgel ( $L_c$ ) and metastable gel ( $L_\beta$ ) phases at low temperatures, lamellar liquid-crystalline phase ( $L_\alpha$ ) at intermediate temperatures, and inverted hexagonal phase ( $H_{II}$ ) at elevated temperatures (1–11). Typical phase sequences in heating scans are  $L_c \rightarrow L_\alpha \rightarrow H_{II}$  or  $L_\beta \rightarrow L_\alpha \rightarrow H_{II}$  depending on the initial state, and  $H_{II} \rightarrow L_\alpha \rightarrow L_\beta$  in cooling direction. It is generally thought that fully hydrated PEs undergo a simple gel( $L_\beta$ )-to-liquid-crystalline( $L_\alpha$ ) phase transition in contrast to fully hydrated phosphatidylcholines (PCs), in which a ripple gel phase ( $P_\beta$ ) appears between the lamellar gel and liquid-crystalline phases. Measurements by high sensitivity differential scanning calorimetry (HSDSC) have led to the conclusion, however, that the  $L_\beta \rightarrow L_\alpha$  transition in diacyl PEs is not a single-peak transition but has a fine structure, particularly well resolved at low scan rates (11). Examination of this transition at a scan rate of 0.1°C/min has shown that the

excess specific heat capacity ( $C_p$ ) vs. temperature curve is a multicomponent curve with a clearly resolved small peak preceding the main endotherm by 0.3–0.4°C on the temperature axis. These peaks are smeared into a single asymmetric transition at a scan rate of 1°C/min. At the same time, the  $L_c \rightarrow L_\alpha$  transition of these lipids is represented by a single asymmetric peak at all scan rates. It has been suggested on basis of these findings that, similarly to PCs, the  $L_\beta \rightarrow L_\alpha$  transition of PEs actually consists of a “pretransition” and a “main transition,” but these two transitions can be resolved as separate peaks only under quasistatic heating conditions (11). Such interpretation implies that the  $L_\beta \rightarrow L_\alpha$  phase transformation proceeds through some intermediate phase which should appear in a narrow temperature window between the  $L_\beta$  and  $L_\alpha$  phases. On the other hand, the detection of such fine structure and/or existence of intermediate phases have not been reported previously in studies using x-ray diffraction methods (6, 9, 10). This disagreement could arise, however, from purely methodological reasons because the temperature resolution of the latter methods is normally much less than that of HSDSC. It is of interest, therefore, to reexamine this transition by x-ray diffraction under temperature control of a high precision, similar to that in calorimetry.

In our previous paper (I.) (reference 12), devoted to the phase behavior of hydrated dipalmitoylphosphatidylcholine (DPPC), we described a method for time-

Haruhiko Yao's present address is Department of Physics, Tokyo Institute of Technology, Meguro-ku, Tokyo 152, Japan.

resolved x-ray diffraction measurements under precise temperature control, comparable to that in calorimetry with respect to temperature uniformity in the sample cell, and employing perfectly constant scan rates in the range 0.05–0.5°C/min. Here we apply this method, in combination with calorimetry, to study the fine structure of the phase transitions in hydrated dipalmitoylphosphatidylethanolamine (DPPE).

## MATERIALS AND METHODS

### Sample preparation

DPPE (1,2-dipalmitoyl-*sn*-glycero-3-phosphorylethanolamine) was purchased from Avanti Polar Lipids, Inc. (Birmingham, AL). For comparison, DPPE (puriss. grade) obtained from Fluka AG (Buchs, Switzerland) was also used in the calorimetric measurements. Both lipids were checked for purity by thin layer chromatography on silicagel plates (Merck, Bracco S. p. A., Milan). The solvent used was chloroform/methanol/water (65:25:4) and the lipid spots were visualized with iodine vapor or with H<sub>2</sub>SO<sub>4</sub>. Such checks were made with fresh lipids and also with lipids after the HSDSC measurements in order to find out whether the high-temperature incubations of the samples in the calorimetric cell leads to noticeable degradation of the lipid. In both cases, single spots of identical positions (*R<sub>f</sub>* values) were displayed on the plates with no traces of impurities and products of lipid degradation. The lipid was dispersed in doubly distilled deionized water (pH 5.3, conductivity less than 2 μS) by vortexing at room temperature. The freeze-thaw procedure described in reference 11 was also used in the HSDSC measurements. In order to examine the effect of pH on the phase transition as monitored by HSDSC, samples at different pH values were prepared in 0.2 M phosphate buffer (NaH<sub>2</sub>PO<sub>4</sub>/NaOH; Merck). The pH values of the buffer solutions were measured before dispersing the lipid with a Radiometer PHM82 pH meter (Copenhagen, Denmark). Their stability to time in the lipid dispersions was checked with paper pH indicators (Merck). The lipid concentrations were 20 wt% in the x-ray measurements, 10 wt% in DSC, and 0.07 wt% in HSDSC. Such dispersions display an L<sub>c</sub> → L<sub>α</sub> transition in the first heating scans and L<sub>β</sub> → L<sub>α</sub> transitions in the successive scans (11). Dispersions incubated at 75°C and vortexed several times at this temperature display L<sub>β</sub> → L<sub>α</sub> transitions in the first heating.

### Calorimetry

HSDSC measurements were made using Privalov DASM-1M and DASM-4 microcalorimeters (Special Bureau of Biological Instrumentation of the Academy of Sciences of the USSR, Moscow) (13) at heating rates of 0.1, 0.5, and 1°C/min. Cooling scans were made with the DASM-4 apparatus at a scan rate of 0.5°C/min. Due to its specific construction and calibration methods, the exact values of peak areas and temperatures cannot be determined in the cooling mode of a DASM-4 apparatus. DSC measurements were made using a Seiko SSC/580 microcalorimeter (Tokyo, Japan) at heating and cooling rates in the range 0.02–0.5°C/min.

The HSDSC measurements did not reveal any systematic difference in the phase behavior of the lipids from the two sources.

### Time-resolved x-ray diffraction

Time-resolved low-angle x-ray experiments were carried out with a small angle synchrotron x-ray diffractometer at station 15A of the

Photon Factory of the National Laboratory for High Energy Physics in Japan. The experimental arrangement and temperature control are described in detail in the previous paper (I.) (reference 12). The accumulation time of the individual diffraction frames was 30 s in all measurements.

## RESULTS

### Differential scanning calorimetry

The purpose of the calorimetric measurements was to reproduce the observations of Chowdhry et al. (11) concerning the complex shape of the L<sub>β</sub> → L<sub>α</sub> phase transition in DPPE. In the first heating scans, nonhydrated dispersions of DPPE heated at 0.1 and 0.5°C/min showed a single asymmetric endotherm broadened toward lower temperatures (L<sub>c</sub> → L<sub>α</sub>). The transition shape and peak temperature were not noticeably affected by the scan rate. The heating was terminated at 1.5°C above the transition. The calorimetric cell was cooled to about 50°C and after that successive heating scans through the L<sub>β</sub> → L<sub>α</sub> transition were made at scan rates in the range 0.1–1°C/min. The effect of pH of a phosphate buffer solution on these transitions is illustrated by Figs. 1 and 2. The transition parameters are summarized in Table 1. A two-peak transition was found only at pH 6.2. A two-peak L<sub>β</sub> → L<sub>α</sub> transition was recorded also in DPPE dispersions in decarbonized bidistilled water (Fig. 3 *b*). It should be strongly emphasized, however, that the two-peak structure was very poorly reproducible in our experiments. Many samples, prepared by the same protocol, displayed single-peak transitions in the place of the two-peak transitions shown in Figs. 1 and 3. Also, no fine structure in the L<sub>β</sub> → L<sub>α</sub> transition could be

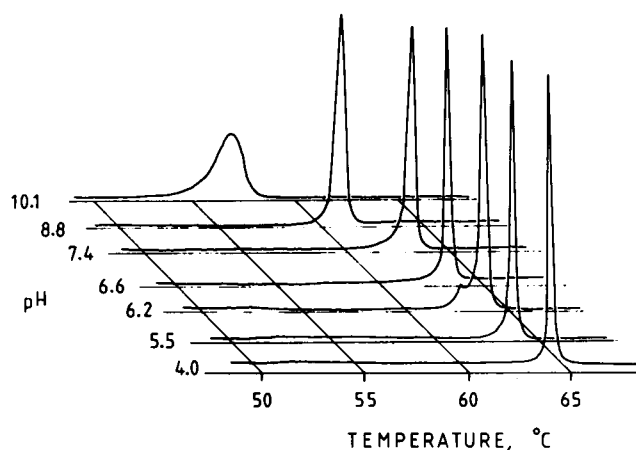


FIGURE 1 High sensitivity DSC scans of the L<sub>β</sub> → L<sub>α</sub> phase transitions in DPPE suspensions in 0.2 M phosphate buffer at differing pH values. Heating rate 0.1°C/min.

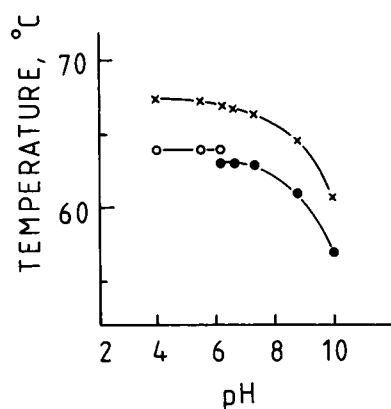


FIGURE 2 pH dependence of the transition temperatures of the  $L_c \rightarrow L_a$  (X),  $(L_p \rightarrow L_a)'$  (O), and  $(L_p-L_a)''$  (●) transitions in DPPE suspensions in 0.2 M phosphate buffer. The respective thermograms are shown in Fig. 1.

detected in DSC measurements of dispersions with 10 wt% of DPPE (data not shown). By varying the ionic strength, pH, and lipid concentration we were unable to find conditions with reproducible two-peak structure of the  $L_p \rightarrow L_a$  transition.

In cooling mode, however, the complex shape of the reverse transition was reproducible and much better resolved by both HSDSC and DSC. Cooling DSC thermograms at scan rates 0.02–0.5°C/min showed two-peak transitions with a shoulder between them suggesting the existence of a third peak (data not shown). The fine structure of the transitions was better resolved in the HSDSC measurements, due presumably to a smaller temperature gradient and higher temperature resolution in the sample cell of the DASM-4 microcalorimeter. A complex transition shape was found in a broad range of pH values in buffer solutions (Fig. 4) and also in bidistilled water (Fig. 5 *b*). It is clear from Figs. 5 *b* and 6 *b* that the complex shape is due to a superposition of at least four different peaks, separated in temperature by few tenths of a degree. There was no relation between

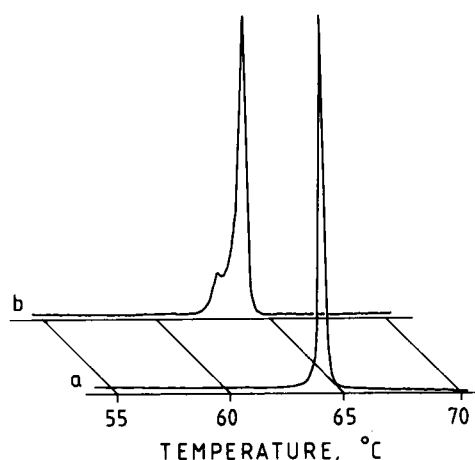


FIGURE 3 High sensitivity DSC scans of the  $L_p \rightarrow L_a$  transitions in DPPE suspensions in distilled water (a) carbonized after several days of storage (pH 4.2), (b) decarbonized under nitrogen (pH 6.8). Heating rate 0.1°C/min.

the shape of the heating and cooling transitions, as illustrated by Fig. 5, where a four-peak cooling transition is preceded by a single-peak heating transition. The shape of the  $L_a \rightarrow L_p$  transition was found to depend strongly, however on the incubation time in the liquid-crystalline phase before the cooling scan (Fig. 6). When the sample was cooled immediately after the heating transition, the fine structure in the cooling transition was almost absent (Fig. 6 *a*). On the other hand, a 30-min incubation in the liquid-crystalline phase resulted in a well resolved four-peak transition shape (Fig. 6 *b*). Incubation times of 30 min at temperatures in the  $L_a$  phase (measurements were carried out for several temperatures up to 80°C) were sufficient for the full development of the fine structure. As stated under the Sample preparation section, no lipid degradation products were detected in the samples by thin layer chromatography after such high temperature incubations. The calorimetry itself also provides a test for the lack of degradation

TABLE 1 Thermodynamic parameters of DPPE phase transitions at different pH determined from HSDSC thermograms

pH	$L_c \rightarrow L_a$			$L_p \rightarrow L_a$			
	$T_m$ °C	$\Delta T_{1/2}$ °C	$\Delta H$ kcal/mol	$T_m$ °C	$\Delta T_{1/2}$ °C	$\Delta H$ kcal/mol	
4.00	67.4	0.48	19.8	63.8	0.22	9.6	
5.50	67.2	0.46	18.2	63.8	0.22	9.3	
6.24	66.8	0.48	19.9	63.8	62.7	0.35	10.2
6.57	66.7	0.51	19.0		62.7	0.28	9.7
7.40	66.3	0.55	17.9		62.5	0.40	9.6
8.80	64.6	0.70	19.2		61.1	0.51	10.3
10.10	60.8	1.58	18.2		57.0	1.56	9.3

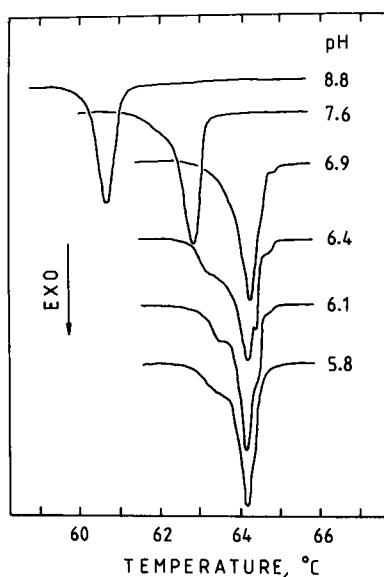


FIGURE 4 Cooling high sensitivity DSC scans through the  $L_\alpha \rightarrow L_\beta$  transition in DPPE suspensions in 0.2 M phosphate buffer at different pH. Cooling rate  $0.5^\circ\text{C}/\text{min}$ .

products, because the heating  $L_\beta \rightarrow L_\alpha$  transitions recorded after a high temperature incubation were always identical to those recorded in unincubated samples. It is therefore clear that the multippeak shape of the  $L_\alpha \rightarrow L_\beta$  transition should be related to a process of slow (on a scale of minutes) restructuring of the  $L_\alpha$  phase.

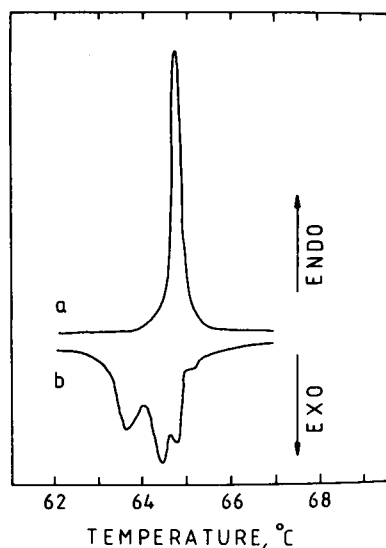


FIGURE 5 A sequence of heating (*a*) and cooling (*b*) HSDSC scans through the  $L_\beta \leftrightarrow L_\alpha$  phase transition of DPPE in distilled water. Scan rate  $0.5^\circ\text{C}/\text{min}$ . In this experiment, pH was 5.3.

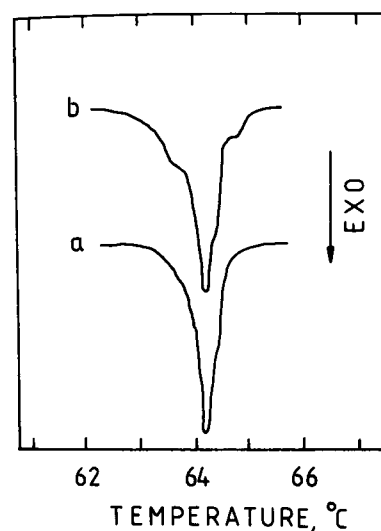


FIGURE 6 Cooling thermograms of the  $L_\alpha \rightarrow L_\beta$  transition of DPPE suspensions in 0.2 M phosphate buffer at pH 6.1. Scan *a* was made immediately after the heating transition, while scan *b* was made after 30 min incubation in the liquid-crystalline phase. Cooling rate  $0.5^\circ\text{C}/\text{min}$ .

Incubation at a constant temperature in this phase results in the appearance of at least four states in the  $L_\alpha$  phase which give rise to the different thermal behavior in cooling direction. Since a multippeak cooling transition is most often preceded, and followed, by a single-peak heating transition, it appears that the "different"  $L_\alpha$  phases finally relax into a "single," homogeneous  $L_\beta$  phase upon cooling.

### Time-resolved low-angle x-ray diffraction

All diffraction measurements were made with DPPE from Avanti Polar Lipids, Inc. Scan rates of 0.1 and  $0.5^\circ\text{C}/\text{min}$  were employed in order to ensure compatibility with the calorimetric results. Between 20 and 55 successive diffraction frames were recorded during temperature scans. With accumulation time of 30 s for each frame, the temperature resolution of these frames was 0.05 and  $0.25^\circ\text{C}$  for the two scan rates, respectively. Fresh samples, which were initially exposed by the incident beam or successively shifted with respect to the initial beam position of the incident beam (12), were used in all scans. Thus, the maximum exposure time did not exceed 30 min except for the measurements at constant temperature shown in Fig. 9. For the lack of a principal difference between the results obtained at the two above mentioned scan rates, we illustrate here only the measurements made at scan rate of  $0.1^\circ\text{C}/\text{min}$ .

Scans through the  $L_c \rightarrow L_\alpha$  transition,  $L_\beta \rightarrow L_\alpha$  transition, and  $L_\alpha \rightarrow L_\beta$  transition at  $0.1^\circ\text{C}/\text{min}$  are shown in Figs. 7, 8 and 10, respectively. The lamellar periods of the phases were 5.54 nm for the  $L_c$  phase, 5.97 nm for the  $L_\beta$  phase, and 5.22 nm for the  $L_\alpha$  phase, in agreement with the previously reported values (6). The peak intensities of the first-order lamellar reflections are

also shown. It is important to note that the relative changes of peak area and peak intensity during the transitions are identical. Therefore, we can use either the peak intensity variations or the peak area variations in analyzing the data.

Several important conclusions follow from the data shown in Figs. 7–10. All transitions proceed via finite-

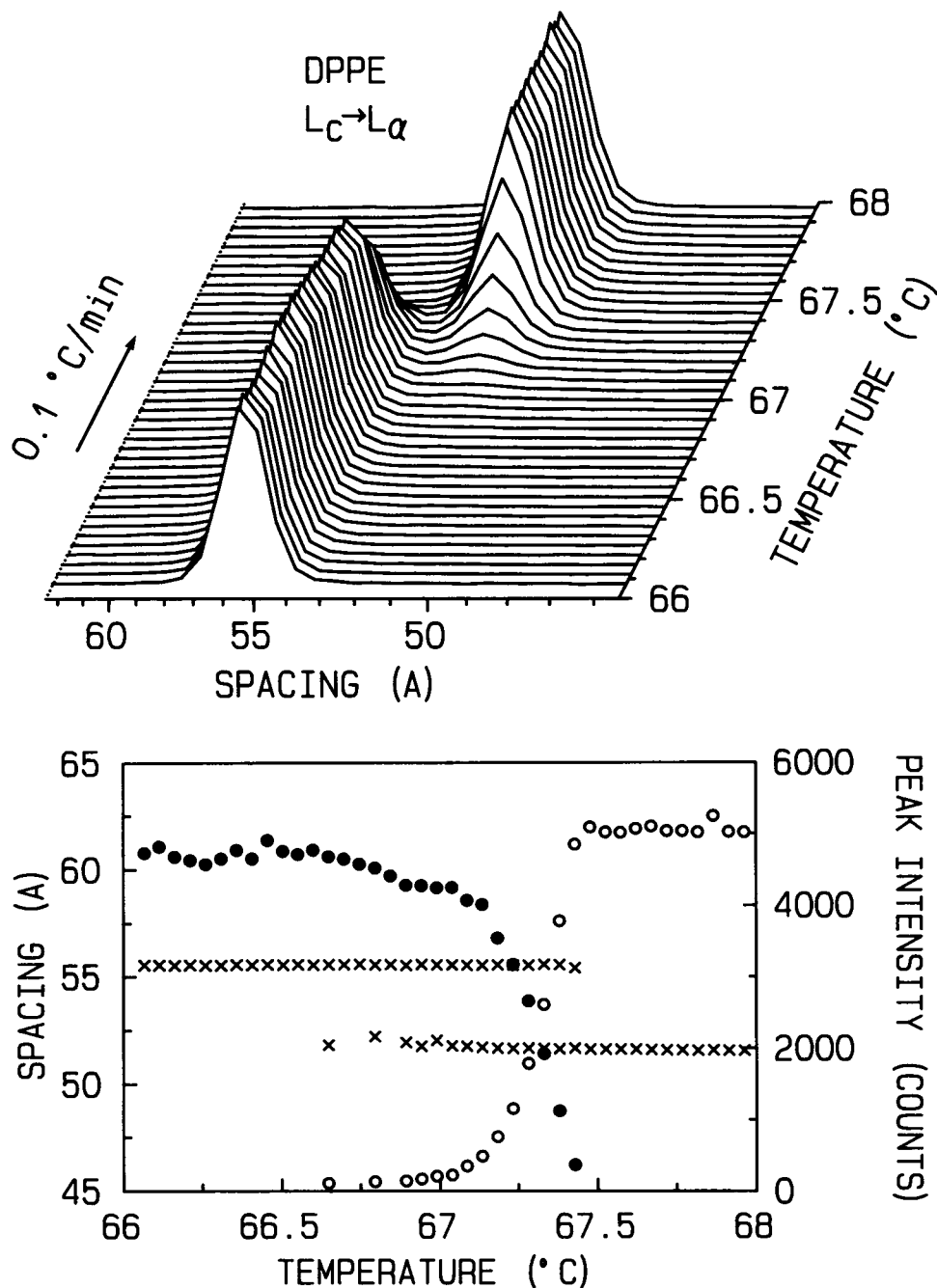


FIGURE 7 The  $L_c \rightarrow L_\alpha$  transition of DPPE in excess water recorded by low angle x-ray diffraction at heating rate  $0.1^\circ\text{C}/\text{min}$ . Spacing (X); peak intensities of the  $L_c$  and  $L_\alpha$  phases (● and ○), respectively. In this experiment, pH was 5.3.

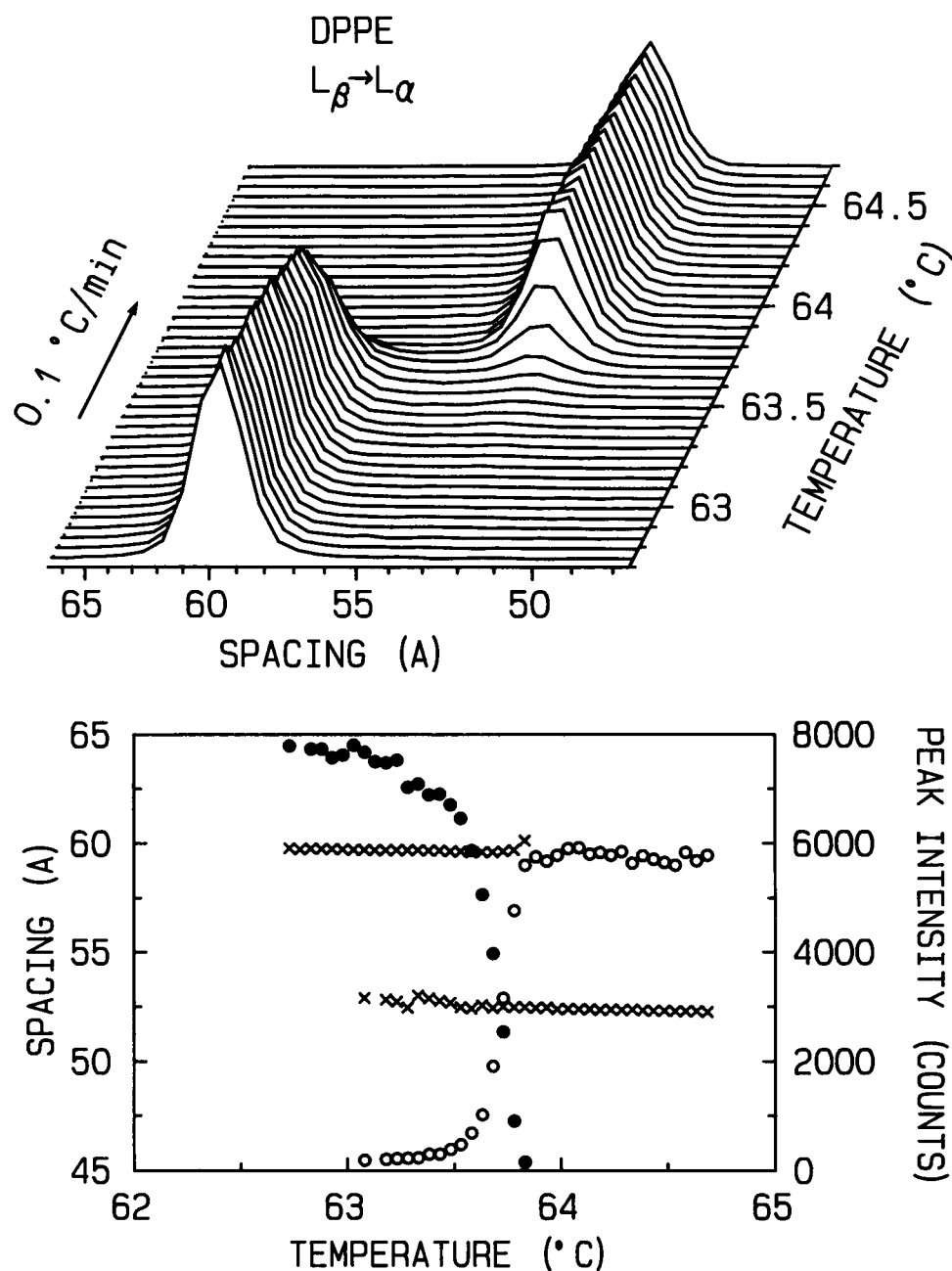


FIGURE 8 The  $L_\beta \rightarrow L_\alpha$  transition of DPPE in excess water recorded by low-angle x-ray diffraction at heating rate  $0.1^\circ\text{C}/\text{min}$ . Spacing (X); peak intensities of the  $L_\beta$  and  $L_\alpha$  phases (● and ○), respectively.

range coexistence of the initial and final phases without detectable intermediate structures. At scan rates  $0.1$  and  $0.5^\circ\text{C}/\text{min}$ , the respective coexistence ranges were  $66.6$ – $67.4^\circ\text{C}$  for the  $L_c \rightarrow L_\alpha$  transition at both scan rates,  $63.0$ – $63.8$  and  $63.3$ – $63.9^\circ\text{C}$  for the  $L_\beta \rightarrow L_\alpha$  transition, and  $63.6$ – $62.5$  and  $63.6$ – $62.2^\circ\text{C}$  for the  $L_\alpha \rightarrow L_\beta$  transition. In all cases, the decrease of the peak intensity of one phase is accompanied with a synchronous increase

of the intensity of the other phase. The sum of the two intensities is almost constant. This shows that there is no significant contribution of hidden states to the intensities during the transitions, and the predominant part is either in the initial or final phase.

In order to check the stability of the phase coexistence during the  $L_\beta \rightarrow L_\alpha$  transition, a heating scan at  $0.1^\circ\text{C}/\text{min}$  was terminated within the transition region at

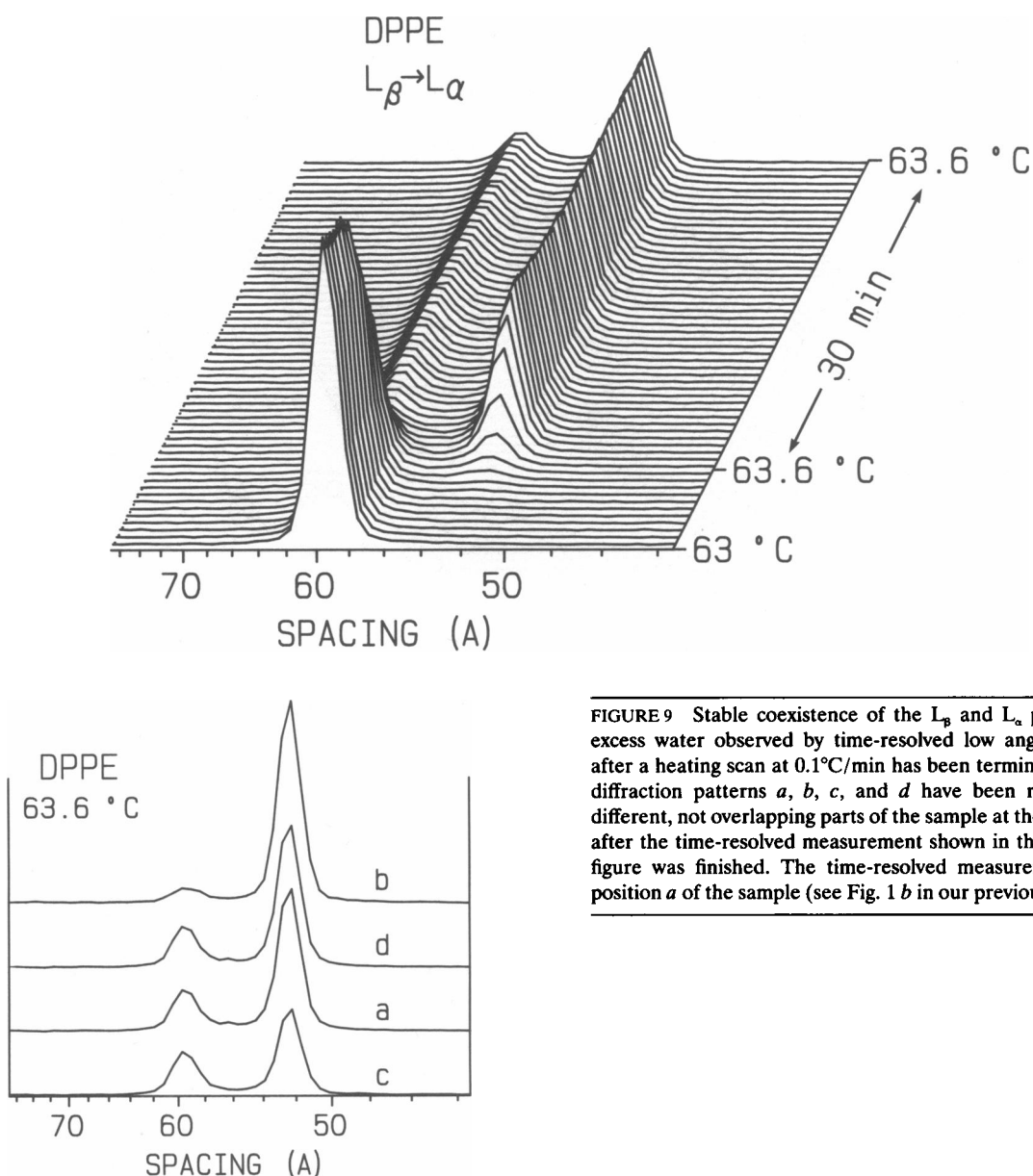


FIGURE 9 Stable coexistence of the  $L_\beta$  and  $L_\alpha$  phases of DPPE in excess water observed by time-resolved low angle x-ray diffraction after a heating scan at  $0.1^\circ\text{C}/\text{min}$  has been terminated at  $63.6^\circ\text{C}$ . The diffraction patterns *a*, *b*, *c*, and *d* have been recorded from four different, not overlapping parts of the sample at the same temperature after the time-resolved measurement shown in the upper part of the figure was finished. The time-resolved measurement was made in position *a* of the sample (see Fig. 1 *b* in our previous paper [12]).

$63.6^\circ\text{C}$  and diffraction patterns were recorded at this temperature for  $\sim 30$  min (Fig. 9, *top*). The ratio of the two coexisting phases did not change during this time. In the same experiment, after the time-resolved measurement shown in Fig. 9 (*upper*), the sample region served for the measurement was shifted with respect to the incident beam position as explained in reference 12, and then diffraction patterns were obtained at four different regions at the same temperature of  $63.6^\circ\text{C}$ , in which each of the regions was chosen so as not to overlap among them (Fig. 9, *lower*). The patterns *a*, *b*, *c*, and *d* correspond to the sample portions denoted by the same letters in Fig. 1 *b* of reference 12. The horizontal and vertical displacements of the sample were 4 and 1.5 mm,

respectively, while the beam cross-section was  $1.6 \times 0.7$  mm (width  $\times$  height). The time-resolved measurement shown in Fig. 9 (*upper*) was made in position *a* of the sample. The measurements at the four different sample positions were made for  $\sim 15$  min. After that the sample was returned to position *a* and the diffraction pattern recorded in this position was identical to that shown in Fig. 9 (*upper*). Thus, the overall time, in which the ratio of the two coexisting phases was kept constant, was more than 40 min. Assuming that the variation of the ratio of the two coexisting phases between sample positions *a*, *b*, *c*, and *d* in Fig. 9 (*lower*) was due to a temperature gradient in the sample, and taking into account the transition width from Fig. 8, it is easy to calculate that

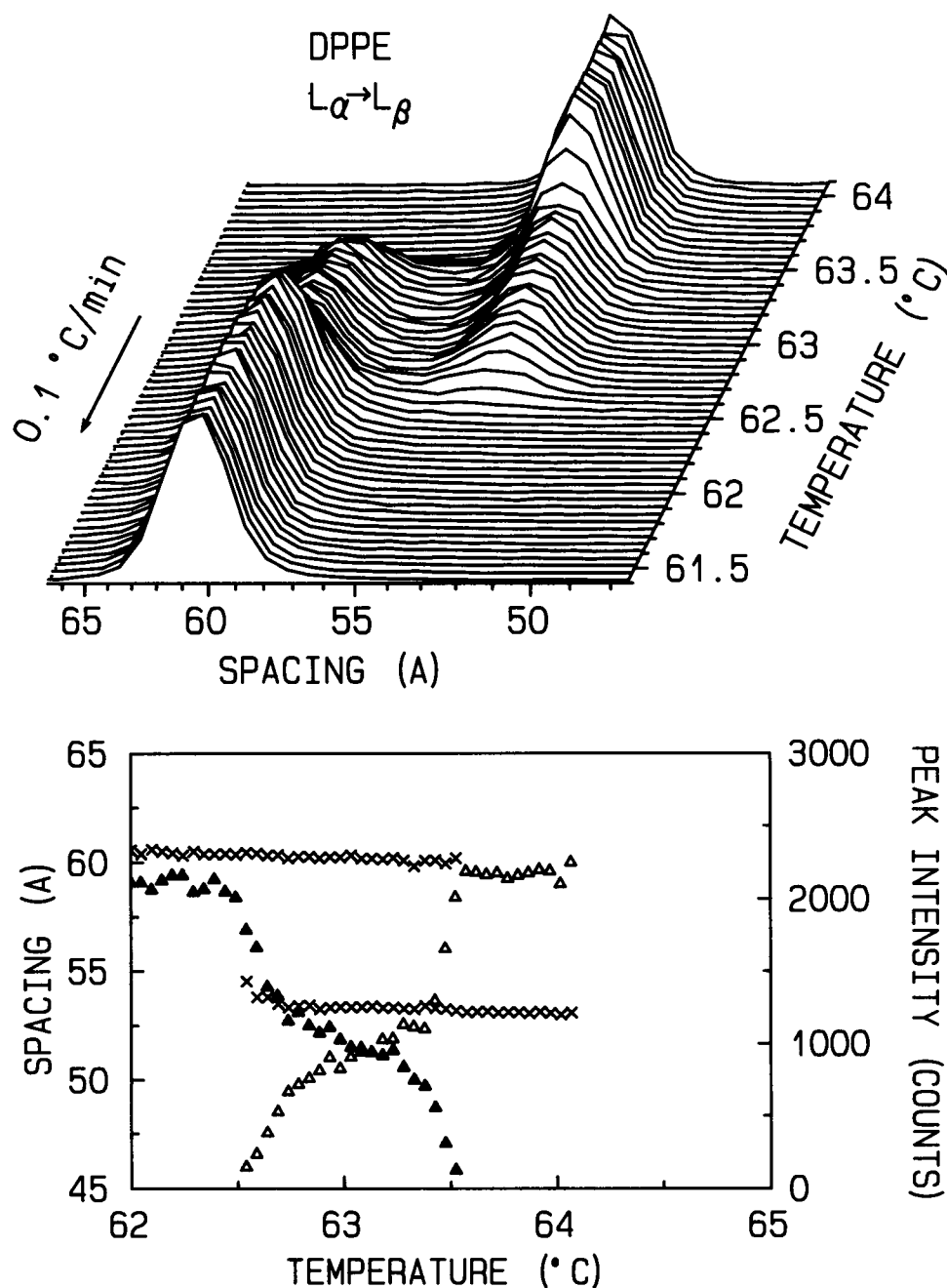


FIGURE 10 Cooling  $L_{\alpha} \rightarrow L_{\beta}$  transition of DPPE in excess water recorded by low angle x-ray diffraction at scan rate  $0.1^{\circ}\text{C}/\text{min}$ . Spacing (X); peak intensities of the  $L_{\beta}$  and  $L_{\alpha}$  phases (▲ and △), respectively. The sample has been incubated in the  $L_{\alpha}$  phase for 15 min before the cooling scan.

the gradient was less than  $0.02^{\circ}\text{C}/\text{mm}$ , perpendicular to the incident beam direction. The measurement illustrated by Fig. 9 is also indicative of the absence of radiation damage after 30-min exposures.

A comparison of the intensity ratios of the gel and liquid-crystalline phases in Figs. 8 and 9 shows that, at constant temperature of  $63.6^{\circ}\text{C}$ , the stable  $L_{\alpha}$  to  $L_{\beta}$  ratio

is significantly greater than the transient value of this ratio at the same temperature during the continuous scan shown in Fig. 8. It is evident from a closer inspection of Fig. 9 that the  $L_{\alpha}$  peak continues to grow in five successive frames (total accumulation time of 150 s) after the temperature scan was stopped at  $63.6^{\circ}\text{C}$ . It is thus clear that the state of stable coexistence of the two



phases in the transition region is preceded by a fairly long (150 s) relaxation taking place at constant temperature after termination of the heating scan in the transition region. It is important to note that this relaxation process cannot be ascribed to a temperature overshoot after termination of the heating scan, because according to the readings of the thermocouple placed adjacent to the sample, the magnitude of the overshoots upon termination of scans at 0.1°C/min was  $\sim 0.015^\circ\text{C}$ , and their duration was less than 30 s. Since these values are of the order of the temperature fluctuations in the sample (12), we conclude that the above noted relaxation is most likely due to a kinetic retardation of the  $L_\beta \rightarrow L_\alpha$  transition in continuous heating scans at 0.1°C/min. As will be shown below, a similar retardation effect is typical also of the cooling  $L_\alpha \rightarrow L_\beta$  transition.

After the measurements at 63.6°C shown in Fig. 9 were completed, the sample was heated up to 64°C at 0.1°C/min and kept at this temperature for 20 min. Two diffraction patterns recorded during this time showed that the lipid was fully converted into the liquid-crystalline phase, in agreement with Fig. 8. After that the sample was cooled back to 63.6°C (this is the onset temperature of the reverse transition according to Fig. 10) at 0.1°C/min and incubated at this temperature for 30 min. Diffraction patterns recorded during this time from different sample parts at  $\sim 5$ -min intervals showed a coexistence of a predominantly liquid-crystalline phase with traces of the gel phase, but no apparent relaxation process. After the 30-min incubation at 63.6°C, the sample was cooled further down to 63.4°C at 0.1°C/min and diffraction patterns were recorded at this temperature from three different sample portions at 3-min intervals. These patterns showed a predominantly gel phase with traces of the liquid-crystalline phase (Fig. 11). Therefore, in this cooling procedure the  $L_\alpha \rightarrow L_\beta$  transformation was almost completed at 63.4°C, while, as evident from Fig. 10, in a continuous cooling scan from 64°C at 0.1°C/min the main part of this transition was below 63.4°C and completed at 62.5°C. This shows a strong influence of kinetic retardations on the transition position and profile in continuous cooling scans at 0.1°C/min.

The temperature dependence of the intensity in Fig. 10 (lower) clearly shows that the cooling  $L_\alpha \rightarrow L_\beta$  transition is not a simple two-state transition, because there are at least two inflection points in the intensity. At the same time, no other phases, except coexisting  $L_\alpha$  and  $L_\beta$  phases, appear in the transition region, because there are only two lamellar spacings corresponding to the  $L_\alpha$  and  $L_\beta$  phases. Thus, the x-ray data are consistent with the calorimetric results concerning the complex shape of the  $L_\alpha \rightarrow L_\beta$  transition. However, there is no evidence indicating the existence of intermediate states

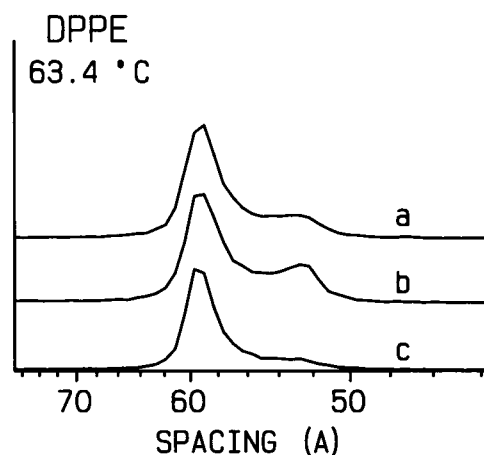


FIGURE 11 Low angle x-ray diffraction patterns of fully hydrated DPPE recorded from three different sample portions at 63.4°C. These patterns have been recorded after cooling of the sample from 64°C at 0.1°C/min and intermediate incubation for 30 min at 63.6°C (see Results for more details).

with lamellar spacings different from those of the  $L_\alpha$  and  $L_\beta$  phases. The results of the x-ray experiment do not explain the complex transition shape in the thermogram.

Preliminary wide-angle x-ray diffraction experiments were performed during the  $L_\beta \rightarrow L_\alpha$  transition at a rate of 0.1°C/min, in which the low angle diffraction profiles were recorded simultaneously (data not shown). In these experiments, the coexistence of the wide-angle diffraction lines of the  $L_\alpha$  and  $L_\beta$  phases coincided with that of the low angle diffraction lines. The detailed behavior in the coexistence region was, however, less clear in comparison with the low angle diffraction because the wide-angle diffraction line of the  $L_\alpha$  phase was broad as usually observed.

## DISCUSSION

The calorimetric measurements in the  $L_\beta \rightarrow L_\alpha$  phase transition of hydrated DPPE at a slow scan rate (0.1°C/min) confirm the existence of the fine structure described by Chowdhry et al. (11), but show that it is very poor in the reproducibility. As noted in Results, we were unable to find conditions ensuring its reproducible observation. Nor was it possible to detect phases, other than coexisting  $L_\beta$  and  $L_\alpha$  phases, in this transition by means of low angle time-resolved x-ray measurements made at the same scan rate of 0.1°C/min. Moreover, the coexisting phases were found to be well correlated and stable for more than 30 min in the transition region (Fig. 9). The x-ray data thus provide a good basis for the conclusion that the  $L_\beta \rightarrow L_\alpha$  phase transition of hydrated

DPPE is a two-state transition characterized by a stable, not "small-scale" but "large-scale" (according to the terminology introduced in reference 12), coexistence of the initial and final phases.

There is little doubt that the reverse  $L_\alpha \rightarrow L_\beta$  transition in hydrated DPPE is a multicomponent transition. This is evident from both calorimetric (Figs. 4–6) and x-ray results (Fig. 10). Under certain conditions, illustrated by Figs. 4–6, at least four peaks can be resolved in this transition. A similarly complex shape of the liquid-crystalline to gel transition has also been observed for unsaturated phosphatidylethanolamines (14). The possibility that the multipeaks reflect a series of transitions between more or less stable intermediate phases appears unlikely, because the data in Fig. 10 show no intermediate phases different from the  $L_\alpha$  and  $L_\beta$  phases although the fine structure is clearly visible. An important finding with respect to the origin of the complex transition profile is illustrated in Fig. 6. It shows that the fine structure of the transition develops when the sample is incubated in the liquid-crystalline phase. It is clear from these experiments that the fine structure of the cooling transition is due to an intrinsic heterogeneity in the  $L_\alpha$  phase, which does not appear immediately after heating from the gel phase, but develops on the scale of minutes upon equilibration of the sample above the transition temperature. In this way, we arrive at the conclusion that the equilibrium state of the  $L_\alpha$  phase of DPPE is represented by a mixture of domains that cannot be distinguished by x-ray scattering, but differ in thermal behavior. The x-ray experiments described under Results and showing that the temperature range of the  $L_\alpha \rightarrow L_\beta$  transition depends on the cooling protocol suggest that this difference (and the resulting complex transition shape) is probably of kinetic origin.

It is worth noting that the relaxation time of 150 s, preceding the establishment of the stable coexistence state in the  $L_\beta$ – $L_\alpha$  transition region (Fig. 9), exceeds by about two orders of magnitude the relaxation (transit) times for this transition measured in temperature jump experiments (see, e.g., the review from reference 15 for a summary). Temperature jumps are usually initiated far below and terminated far beyond the phase transition regions, while our measurement was carried out inside the transition region at a temperature and was reached by means of a slow scan. It is clear that in both fast and slow temperature scans the phase transformation proceeds along nonequilibrium pathways determined by the rate of temperature increase. An abrupt termination of a temperature scan at a given temperature would produce a relaxation time specific for the nonequilibrium state reached at that time and corresponding to the equilibrium state at the temperature. Besides the obvious dependence on the temperature protocol, the com-

paratively large value of 150 s demonstrates, in accord with the results described in reference 12, that the relaxation times increase significantly when the temperature approaches the transition midpoint. In their studies on the kinetics of the phase transitions in phosphatidylcholines, Tsong and Kanehisa (16) and Van Osdol et al. (17) also detect a great enhancement of the relaxation times around the transition midpoints.

Especially at alkaline pH values, the peak temperatures and transition widths of the DPPE transition are rather sensitive to the pH value of the buffer solution (Figs. 1–3 and Table I). As shown in earlier reports, these effects are associated with pH-induced deprotonation of the lipid polar group and respective changes in the surface electric charge (18, 19). The electrophoretic measurements of Bangham et al. (20) have demonstrated that PE aggregates in aqueous systems are negatively charged over the whole range of pH values above 2.5. Considering the DPPE multilayers as mixtures of protonated and deprotonated lipid molecules, it seems possible, at least in principle, that the complex thermal behavior reported here is associated with specific, nonuniform distributions of the electrically neutral (zwitterionic) and charged molecules. An investigation of this possibility requires, however, methods different from those used in this work.

The authors thank Dr. S. Matuoka and Dr. S. Kato for valuable discussions in the analysis of x-ray data.

One of the authors (H. Yao) is indebted to the support by a Grant-in-Aid for Encouragement of Young Scientists from the Ministry of Education, Science and Culture of Japan. One of the authors (I. Hatta) is indebted to the support by a Grant-in-Aid for General Scientific Research from the Ministry of Education, Science and Culture of Japan. This work has been performed under the approval of the Photon Factory Program Advisory Committee in Japan (Proposal No. 89-060).

Received for publication 2 May 1991 and in final form 22 October 1991.

## REFERENCES

1. Hitchcock, P. B., R. Mason, K. M. Thomas, and G. G. Shipley. 1974. Structural chemistry of 1,2-dilauroyl-DL-DPPE. Molecular conformation and intermolecular packing of phospholipids. *Proc. Natl. Acad. Sci. USA*. 71:3036–3040.
2. Harlos, K., and H. Eibl. 1980. Influence of calcium on PE. An investigation of the structure at high pH. *Biochim. Biophys. Acta*. 601:113–122.
3. McIntosh, T. J. 1980. Differences in hydrocarbon chain tilt between hydrated PE and PC bilayers: a molecular packing model. *Biophys. J.* 29:237–246.
4. Harlos, K., and H. Eibl. 1981. Hexagonal phases in phospholipids with saturated chains: PE's and phosphatidic acid. *Biochemistry*. 20:2888–2892.

5. Seddon, J. M., G. Cevc, and D. Marsh. 1983. Calorimetric studies of the gel-fluid ( $L_{\beta}$ - $L_{\alpha}$ ) and lamellar-inverted hexagonal ( $L_{\alpha}$ - $H_{II}$ ) phase transitions in dialkyl- and diacylphosphatidylethanolamines. *Biochemistry*. 22:1280-1289.
6. Seddon, J. M., G. Cevc, R. D. Kaye, and D. Marsh. 1984. X-ray diffraction study of the polymorphism of hydrated diacyl- and dialkylphosphatidylethanolamines. *Biochemistry*. 23:2634-2644.
7. Mantsch, H. H., S. C. Hsi, K. W. Butler, and D. G. Cameron. 1983. Studies on the thermotropic behavior of aqueous PE's. *Biochim. Biophys. Acta*. 728:325-330.
8. Chang, H., and R. M. Epand. 1983. The existence of a highly ordered phase in fully hydrated DLPE. *Biochim. Biophys. Acta*. 728:319-24.
9. Caffrey, M. 1985. Kinetics and mechanism of the lamellar gel/lamellar liquid-crystal and lamellar/inverted hexagonal phase transition in PE: a real-time x-ray diffraction study using synchrotron radiation. *Biochemistry*. 24:4826-4844.
10. Tenchov, B., L. Lis, and P. Quinn. 1988. Structural rearrangements during crystal-liquid crystal and gel-liquid crystal phase transitions in aqueous dispersions of dipalmitoylphosphatidylcholine. A time-resolved x-ray diffraction study. *Biochim. Biophys. Acta*. 942:305-314.
11. Chowdhry, B. Z., G. Lipka, A. W. Dalziel, and J. M. Sturtevant. 1984. Multicomponent phase transitions of diacylphosphatidylethanolamine dispersions. *Biophys. J.* 45:901-904.
12. Tenchov, B. G., H. Yao, and I. Hatta. 1989. Time-resolved x-ray diffraction and calorimetric studies at low scan rates. I. Fully hydrated DPPC and DPPC/water/ethanol mixtures. *Biophys. J.* 56:757-768.
13. Privalov, P. L. 1980. Scanning calorimeters for studying macromolecules. *Pure Appl. Chem.* 52:449-497.
14. Epand, R. M., and R. F. Epand. 1988. Kinetic effects in the differential scanning calorimetry cooling scans of phosphatidylethanolamines. *Chem. Phys. Lipids*. 49:101-104.
15. Caffrey, M. 1989. The study of lipid phase transition kinetics by time-resolved x-ray diffraction. *Annu. Rev. Biophys. Biophys. Chem.* 18:159-186.
16. Tsong, T. Y., and M. I. Kanehisa. 1977. Relaxation phenomena in aqueous dispersions synthetic lecithins. *Biochemistry*. 16:2674-2680.
17. Van Osdol, W., R. Biltonen, and M. Johnson. 1989. Measuring the kinetics of membrane phase transitions. *J. Biochem. Biophys. Meth.* 20:1-46.
18. Eibl, H., and P. Woolley. 1979. Electrostatic interactions at charged lipid membranes. Hydrogen bonds in lipid membrane surfaces. *Biophys. Chem.* 10:261-271.
19. Stumpel, J., K. Harlos, and H. Eibl. 1980. Charge-induced pretransition in phosphatidylethanolamine multilayers. *Biochim. Biophys. Acta*. 599:464-472.
20. Bangham, A. D., M. W. Hill, and N. G. A. Miller. 1974. Preparation and use of liposomes as models of biological membranes. *Methods Membr. Biol.* 1:1-68.